

depended upon the relative delay of the 308- and 757-nm pulses. An explanation was afforded by the observation that the 308-nm beam undergoes spectral broadening from self-phase modulation (SPM) in the optical elements in its beam path and, due to the presence of dispersion in these elements, becomes stretched in time and linearly chirped. Overlapping the comparatively shorter 757-nm pulse with the early part of the stretched 308-nm pulse produces a red shift in the  $2\omega_1 - \omega_2$  output beam. Overlapping the 757-nm pulse with the latter portion of the 308-nm pulse produces a blue shift. Exactly this behavior is observed (Fig. 1).

Amplification of the 193-nm seed pulses was measured in a standard, ArF excimer gain module with a 40-cm long discharge region (Lambda-Physics EMG 102). With  $\sim 0.2$ - $\mu$ J pulses applied at the input window of the excimer gain module,  $\sim 20$ - $\mu$ J pulses were obtained at the output end in a single pass, corresponding to a small-signal gain  $>100$ , which is approximately that reported for conventional nanosecond pulses. Reflecting this output back through the excimer gain module in a second pass resulted in a short-pulse energy content of  $\sim 300$   $\mu$ J. This observed drop by more than a factor of 6 in the small-signal gain during the second pass most likely indicates the existence of nonlinear loss in ArF and points to a possible limitation of this system for ultrashort pulse amplification. We also noted a striking, rapid formation of deep-blue color centers in excimer gain module windows made of  $\text{CaF}_2$  or  $\text{MgF}_2$  upon 193-nm short pulse irradiation. We found  $\text{BaF}_2$  windows to be free of the above-mentioned defect, and we now employ this material for this application instead.

A cross-correlation measurement of the amplified pulse width after two passes through the ArF excimer gain module was performed. The amplified 193-nm pulses were temporally overlapped with 308-nm pulses, and both were then focused into a cell containing  $\approx 1$  atm of Xe. The intensity of the  $2\omega_1 - \omega_2$  generated beam at 757 nm was then recorded as a function of the relative delay of the 308- and 193-nm input pulses. The resulting cross-correlation is shown in Fig. 2(a). Speculating that the observed secondary pulse structure resulted from the formation of 0 $\pi$  pulses produced by coherent interaction of the 193-nm short pulse with the Schumann-Runge  $\text{O}_2$  bands that it spectrally overlaps (Fig. 1), we flushed most of the  $\approx 7$ m path length traversed in air by the 193-nm pulses with  $\text{N}_2$  gas. The cross-correlation signal then appeared as in Fig. 2(b), i.e., essentially as a single unstructured pulse. Deconvoluting from this signal the 308-nm pulsewidth (which due to group velocity dispersion had a measured duration of 380 fs at the point where the pulse was injected into the cross-correlator), one deduces that the amplified 193-nm pulse width was  $\sim 320$  fs. Normal dispersion can reasonably account for the observed increase in width over the 150-fs value expected at the output window of the seed-generating cell.

#### 9:45 am

#### CWD7 Femtosecond pulse amplification up to 25 $\mu$ J at 1.5 $\mu$ m

G. Sucha, S. Bolton, D.S. Chemla, *Lawrence Berkeley Laboratory, 1 Cyclotron Rd., Berkeley, CA 94720.*

NaCl F-centers<sup>1</sup> have been shown to be a very good medium for generation of femtosecond pulses near 1.5  $\mu$ m. Due to its very broad gain bandwidth, NaCl combines the capability of femtosecond pulse generation with tunability. Recently, NaCl has been shown to be an excellent medium for amplification as well.<sup>2</sup> In this earlier work, femtosecond pulses from an additive-pulse mode-locked (APM) NaCl laser were amplified to the 5- $\mu$ J level in a three-pass NaCl amplifier, thus enabling continuum generation near 1.5  $\mu$ m. However, due to the long gain lifetime (150 ns) several pulses were amplified in the pulse train. This not only limits the amount of energy which can be extracted in a single pulse (as saturation occurs), it also makes clean experiments difficult. We report the amplification of a single 150-fs pulse to energies 20  $\mu$ J, at a wavelength of 1.55  $\mu$ m.

The layout of the amplifier system is shown in Fig. 1. It employs a simple four-pass noncollinear geometry which is similar to a bowtie amplifier.<sup>3</sup> The gain medium is a  $6 \times 6 \times 15$  mm NaCl crystal which is held at 77 K in a liquid nitrogen cryostat. The crystal is pumped along the 15-mm dimension by a Q-switched Nd:YAG laser ( $\lambda = 1.06$   $\mu$ m) which produces pulses with energies of 1.7 mJ and 80-ns duration at a 1-kHz repetition rate. A single-pass gain of 20 is usually obtained from this crystal, but values as high as 35 have been observed. Auxiliary radiation (which is necessary to counteract orientational bleaching) is provided by the 514-nm line of an air-cooled argon laser.

This multipass amplifier is injected with 150-fs pulses (energy  $\sim 1$  nJ) from an NaCl APM laser through a Faraday isolator and a Pockels cell switchout.<sup>4</sup> With the switchout disabled and opened, the pulses in the amplified train are clearly visible in Fig. 2(a). The 13-ns spacing between pulses corresponds to the 76-MHz repetition rate of the APM oscillator. With the switchout activated, a single pulse is injected into the amplifier. The resulting pulse is shown in Fig. 2(b). Approximately 3 or 4 postpulses are also visible in Fig. 2(b) which are twenty times weaker than the main pulse. The contrast ratio can be improved with more careful adjustment of the Pockels cell voltage and the addition of a saturable absorber. Note that the nearest postpulse is greatly suppressed due to gain saturation by the main pulse. Note also that the main pulse contains more energy than the strongest pulse in the train in Fig. 2(a), indicating that gain saturation is occurring. Maximum energies of 25  $\mu$ J have been obtained in the main pulse. A fifth pass through the crystal does not significantly increase the pulse energy. Currently the extractable pulse energy is limited, in part, by saturation and also by beam distortion from internal crystal inhomogeneities.

Fig. 3 shows autocorrelations of the injected pulse, and the amplified pulse. No measurable pulse broadening occurs in this amplifier, because of the low material dispersion of the amplifier components (glass, NaCl, and  $\text{LiNbO}_3$ ) at the 1.5- $\mu$ m wavelength. These high-power short pulses have been used to generate a strong, femtosecond continuum in various pieces of glass ranging in thickness from 3 to 20 mm. The very broad range of continuum generation (400 nm to beyond 3  $\mu$ m) makes this a useful source for infrared femtosecond spectroscopy.

1. E. Georgiou, J.F. Pinto, and C.R. Pollock, *Phys. Rev. B* **35**, 7636 (1987).
2. C.P. Yakymyshyn, J.F. Pinto, and C.R. Pollock, *Opt. Lett.* **14**, 629 (1989).
3. G. Sucha, and D.S. Chemla, *Opt. Lett.* **16**, 1177 (1991).
4. W.H. Knox, M.C. Downer, R.L. Fork, and C.V. Shank, *Opt. Lett.* **9**, 552 (1984).

Wednesday

May 13, 1992

CONVENTION CENTER ROOM C1

8:00 am Waveguide Lasers

Clifford R. Pollock, *Cornell University, President*

8:00 am

CWE1 Ion implanted channel waveguide lasers

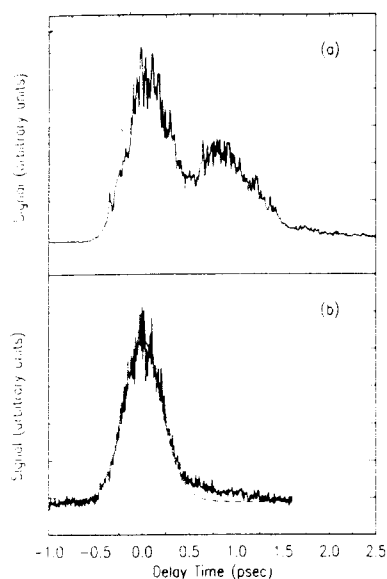
A. C. Large, S. J. Field, D. C. Hanna, D. P. Shepherd, A. C. Tropper, P. J. Chandler,\* P. D. Townsend,\* L. Zhang,\* *Department of Physics and Optoelectronics Research Centre, University of Southampton, Southampton SO9 5NH, U.K.*

We report what we believe to be the first laser operation of channel waveguides formed in Nd-doped crystals by high energy ion implantation. Recently, there has been much interest shown in the fabrication of waveguides by various methods in crystal laser hosts.<sup>1-5</sup> Many crystal host laser systems with interesting features, including broad tunability, upconversion, and large nonlinear and/or electro-optic coefficients, could be operated with lower threshold powers when in the form of a waveguide. The ion implantation method has the particular advantage that it can be used to create waveguides in a wide range of crystals by modifying the refractive index at the crystal surface.<sup>6</sup>

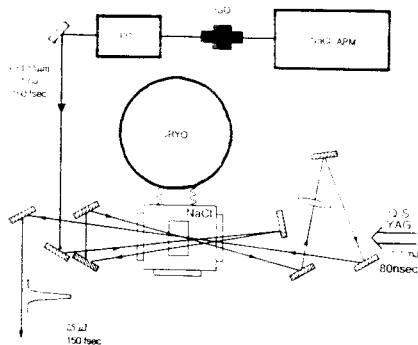
The first materials to be made into channel waveguide lasers by ion implantation are Nd:YAG and Nd:GGG, both of which have been made into planar waveguide lasers by the same method.<sup>12</sup> Fabrication of channels depends on the production of a gold mask on top of the

\*School of Mathematical & Physical Sciences, University of Sussex, Brighton BN1 9QH, U.K.

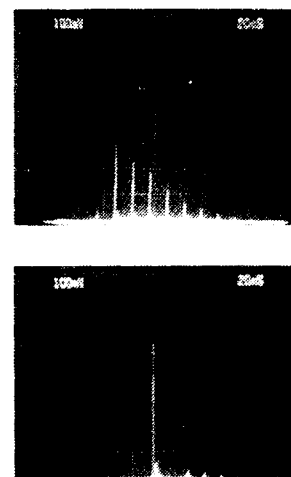
1. S. Szatmari and F.P. Schafer, *J. Opt. Soc. Am. A* **6**, 1877 (1989).



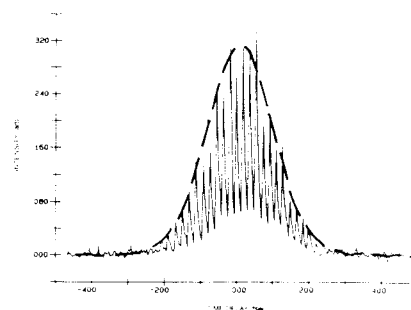
CWD6 Fig. 2. Cross-correlation signal produced at 757 nm ( $2\omega_1 - \omega_2$ ) as a function of relative delay of 308-nm ( $\omega_1$ ) and amplified 193-nm ( $\omega_2$ ) pulses with (a) all 193-nm beams passing through air, (b) all 193-nm beams passing mostly ( $\approx 90\%$ ) through Ni-flushed enclosures. In (b), the dashed curve shows the fit to a cross-correlation with a 380-fs sech<sup>2</sup> pulse (see text) at 308 nm and a 320-fs sech<sup>2</sup> pulse at 193 nm.



CWD7 Fig. 1. NaCl amplifier schematic showing NaCl APM oscillator, Faraday isolator (ISO), Pockels cell switchout (PC), and four-pass amplifier.



CWD7 Fig. 2. Amplified pulse train (a) with switchout opened and disabled. Single amplified pulse (b) with single-pulse injection into amplifier (switchout activated).



CWD7 Fig. 3. Autocorrelations of the injected pulse (dashed) and the amplified pulses (solid). The spiked appearance of the amplified autocorrelation is due to the fast sweep speed of the delay arm relative to the 1-kHz rep-rate of the amplifier. The autocorrelation width corresponds to a pulsewidth of 143 fs assuming sech<sup>2</sup> pulses.

crystal to stop implantation in certain regions. This is made by electroplating 3  $\mu\text{m}$  of gold onto a Ni/Cr layer which has been patterned with photoresist to prevent plating in the regions above where the channels will be formed. The surface is then implanted with  $\text{He}^+$  ions to create channels as shown in Fig. 1. For Nd:YAG an index increase of 0.2% can be obtained at the crystal surface and for Nd:GGG one of 0.06%. This is sufficient to confine the light in two dimensions. In both cases a range of channels from 4–20  $\mu\text{m}$  was formed.

To operate the channels as lasers thin mirrors had to be butted to the ends of the crystal. The pump light (from a 100-mW laser diode) was coupled in using a microscope objective. Using this arrangement the two materials were characterized. The Nd:YAG channels had typical losses of  $\sim 1.5$  dB/cm. For a 2.5-mm crystal length and HR mirrors a threshold of 1.3 mW incident on the launch objective was obtained. Assuming a 70% launch efficiency this corresponds to an absorbed power threshold of  $\sim 500$   $\mu\text{W}$  and compares well to the calculated threshold of 400  $\mu\text{W}$ . With a 17% output coupler the threshold rose to 1.6 mW with a slope efficiency of 29%.

Performances for the Nd:GGG channels were similar to those of Nd:YAG with losses of  $\sim 1$  dB/cm. For a 2.5-mm long channel with HR mirrors the absorbed power threshold was 1.9 mW and with a 17% output coupler the slope efficiency was 27%. The crystal also worked in an extended cavity configuration with the waveguide output collimated using a microscope objective onto the output mirror. An absorbed power threshold of 8 mW was obtained for a 9-mm long crystal.

Ion implantation has been shown to be a versatile technique for creating channel waveguides in crystal laser hosts. Future work on confining the waveguide modes more tightly and reducing the losses could significantly improve these results. With an extended cavity allowing for the insertion of intracavity tuning elements there is now a real possibility of low threshold (diode-pumped) tunable laser operation in various  $\text{Cr}^{3+}$ -doped materials or other tunable systems.

8:15 am

### CWE2 High efficiency amplification and low threshold lasing at 0.8 $\mu\text{m}$ in a thulium-doped fluorozirconate fiber

J.N. Carter, R.G. Smart\*, A.C. Tropper, D.C. Hanna, S.T. Davey, D. Szebesta, Optoelectronics Research Centre, University of Southampton, Southampton SO9 5NH, U.K.

Monomode Tm-doped fluorozirconate fiber can exhibit high gain amplification with pump and signal wavelengths both in the AlGaAs diode range. This is of great potential interest for local area networks operating near 0.8  $\mu\text{m}$ , where transmitters and receivers are significantly less expensive than those at 1.3 or 1.5  $\mu\text{m}$ . In this paper we describe a Tm<sup>3+</sup>-doped fluorozirconate fiber acting when pumped at 785 nm both as an amplifier giving 20-dB gain at 806 nm and as a fiber laser.

The Tm<sup>3+</sup> ion in fluorozirconate (ZBLAN) glass has a strong absorption band at 790 nm corresponding to the  $^3F_4 \rightarrow ^3F_6$  transition. Approximately 88% of ions excited to the  $^3F_4$  level relax radiatively back to the ground state. The peak of this emission is at 805 nm. By contrast, in Tm<sup>3+</sup>-doped silica fibers, essentially all ions excited to the  $^3F_4$  level decay nonradiatively via multiphonon emission to the  $^3H_6$  level as a result of the higher phonon energies in this host, which means that a high gain 0.8- $\mu\text{m}$  amplifier based on a Tm<sup>3+</sup>-doped silica fiber is not achievable.

A 3-m length of 1000-ppmw Tm<sup>3+</sup>-doped ZBLAN fiber of core diameter 3.5  $\mu\text{m}$  was used for the amplifier. The pump source was a Ti:sapphire laser providing power at 785 nm. The signal was provided by a second tunable Ti:sapphire laser, the output power of which was attenuated to  $\sim 10$   $\mu\text{W}$  to allow the measurement of small-signal gain. Pump and signal beams were combined using a polarization rotator and polarizing beam splitter and launched copropagating into the fiber. The ratio of the transmission of the signal when the pump beam was blocked and unblocked was measured, and the host absorption (determined by a cutback) subtracted from this value to give the small-signal gain. Amplification was observed between 800 and 830 nm (Fig. 1 and 2), with a gain of 23 dB at 806 nm for 50 mW of launched pump power.

Modeling of the performance of this amplifier using a numerical method has been undertaken and is in excellent agreement with the experimental results obtained.

Lasing was observed in a resonator formed by butting a  $>99\%$  reflecting mirror against the input end of the fiber and using the 4% Fresnel reflection at the output end to complete the cavity. The lowest threshold observed was 15-mW launched pump power achieved using a 2-m fiber length. Shorter fibers absorbed the pump less efficiently, and in longer fibers the three-level transition was not saturated over the full length, leading to

higher thresholds in either case. For lengths in the 2–3-m range slope efficiencies between 60 and 70% with respect to launched pump power were measured.

This laser has the potential to be operated as a diode-pumped short pulse source. The long metastable level lifetime (1.1 ms) should enable high peak powers (several watts) to be achieved using a single stripe AlGaAs diode-pump laser.

8:30 am

### CWE3 Laser operations of Nd<sup>3+</sup>-doped fiber in a double Fox-Smith geometry

P. Le Boudec, P.L. Francois, F. Sanchez, G.M. Stephan, CNET-LAB/OCM-F, Route de Tregastel, F-22300 Lannion, France

Rare earth-doped fibers are usually inserted in Fabry-Perot resonators yielding highly multimode operation because of both long cavity lengths and large fluorescence spectra. Spectral selectivity can be achieved either by including bulk elements inside the cavity or through coupling of several cavities (Vernier effect). A new cavity based on this effect has been recently proposed to obtain single-longitudinal-mode operation. A double Fox-Smith resonator, composed of two optical fiber couplers was used. The huge advantage of this method is to allow a compact and efficient all-fiber device.

This paper reports laser operations of Nd<sup>3+</sup>-doped fiber used in a double Fox-Smith geometry. Continuous-wave single-longitudinal-mode operation as well as Q-switch operation are demonstrated.

The experimental setup is presented in Fig. 1. An argon laser is used to optically pump the rare earth-doped fibers. A polarizer and a quarterwave plate prevent optical feedback toward the pump laser. The cavity is composed of two dopant optical fiber couplers leading to an all-doped-fiber device. The double Fox-Smith resonator was optimized according to the theory developed in Ref. 2. T mode selectivity in this system is based on the Vernier effect which appears in coupled cavities.

The optimization of the cavity has led to single-longitudinal-mode operation with a low threshold ( $\sim 50$  mW launched). An external Fabry-Perot analyzer was used to verify that the laser oscillates in one longitudinal mode. A delayed self-heterodyne interferometer was built to measure the spectral width of the laser output. The laser linewidth was found to be  $\sim 50$  kHz.

Q-switch operation has been performed by modulation of the losses of the double Fox-Smith cavity with the PZT. Pulse operation has been achieved for a frequency modulation of  $f \approx 1$  kHz (Fig. 2). The pulse duration has been measured to be 1.5  $\mu\text{s}$ .

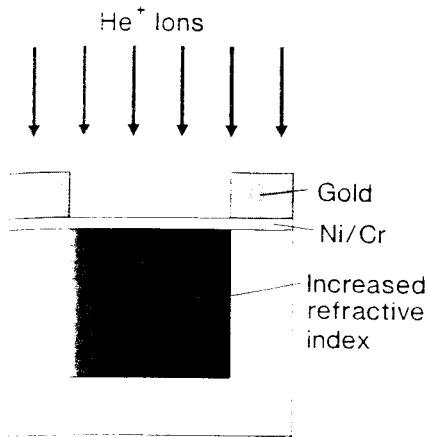
\*Laboratoire d'Optique, ENSSAT, 6, rue de Keraampont, F-22305 Lannion CEDEX, France.

1. P. Urquhart, "Review of rare-earth doped fibre lasers and amplifiers," *IEE Proc.* **135**, Pt.J, 385–407 (1988).
2. F. Sanchez, "Matrix algebra for all-fiber optical resonators," *J. Lightwave Technol.*, **LT-9**, 838–844 (1991).

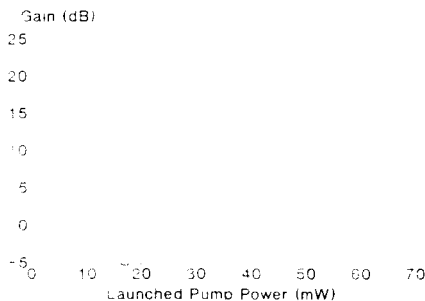
\*Current address: AT&T Bell Laboratories, Crawford Hill Laboratory Holmdel NJ 07733.

\*British Telecom Laboratories, Martlesham Heath, Ipswich IP5 7RE, U.K.

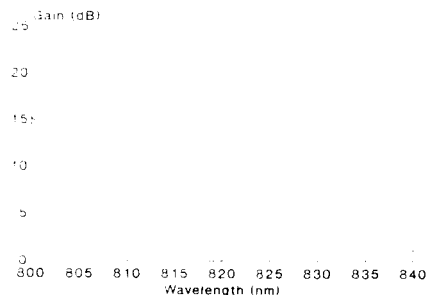
1. S. J. Field, D. C. Hanna, D. P. Shepherd, A. C. Tropper, P. J. Chandler, P. D. Townsend, and L. Zhang, *IEEE J. Quantum Electron.* **QE-27**, 428 (1991).
2. S. J. Field, D. C. Hanna, A. C. Large, D. P. Shepherd, A. C. Tropper, P. J. Chandler, P. D. Townsend, and L. Zhang, *Opt. Comm.* **86**, 161 (1991).
3. S. J. Field, D. C. Hanna, D. P. Shepherd, A. C. Tropper, P. J. Chandler, P. D. Townsend, and L. Zhang, *Opt. Lett.* **16**, 481 (1991).
4. E. Lallier, J. P. Pocholle, M. Papuchon, M. de Micheli, M. J. Li, Q. He, D. B. Ostrowsky, C. Grezes-Besset and E. Pelletier, *IEEE J. Quantum Electron.* **QE-27**, 618 (1991).
5. R. Brinkmann, W. Sohler, and H. Suche, *Electron. Lett.* **25**, 985 (1991).
6. P. D. Townsend, *Rep. Prog. Phys.* **50**, 501 (1987).



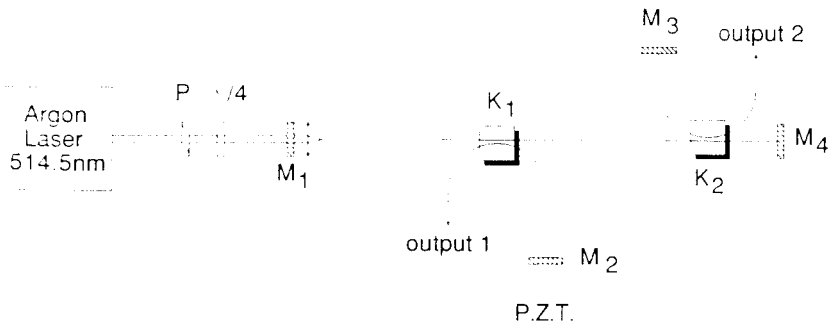
CWE1 Fig. 1. Channel formation.



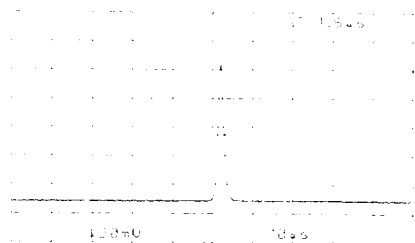
CWE2 Fig. 1. Gain (dB) vs launched pump power (mW).



CWE2 Fig. 2. Gain (dB) vs wavelength (nm).



CWE3 Fig. 1. Details of the double Fox-Smith laser. The argon laser operates at  $\lambda = 514.5$  nm.  $P$ , polarizer;  $\lambda/4$ , quarterwave plate;  $K_1$  and  $K_2$ , optical-doped fiber couplers (coupling ratio = 0.5 at  $\lambda = 1.08$   $\mu$ m);  $M_1$  and  $M_3$ , high reflective bulk mirrors ( $R = 99.5\%$  at  $\lambda = 1.08$   $\mu$ m and  $T = 90\%$  at  $\lambda = 514.5$  nm);  $M_2$  and  $M_4$ , chemically deposited mirrors ( $R = 95\%$  at  $\lambda = 1.08$   $\mu$ m).  $M_2$  is mounted on a PZT to allow the adjustment of the cavity.



CWE3 Fig. 2. Q-switch operation of the double Fox-Smith laser; loss modulation leads to a pulsed laser. The pulse duration is 1.5  $\mu$ s.